Universities of Leeds, Sheffield and York
http://eprints.whiterose.ac.uk/

Published paper

Robinson, V.L., Hunter, C.L., Ward, M.D. (2010) *An improved synthesis, crystal structures, and metallochromism of salts of [Ru(tolyl-terpy)(CN)(3)](-,* Inorganica Chimica Acta, 363 (12), pp. 2938-2944
http://dx.doi.org/10.1016/j.ica.2010.03.021

For *Inorganica Chimica Acta:* Special issue in honour of Prof Animesh Chakravorty

1

An improved synthesis, crystal structures, and metallochromism of salts of [Ru(tolyl-terpy)(CN)₃]⁻

Voirrey L. Robinson, Christopher A. Hunter and Michael D. Ward**

Department of Chemistry, University of Sheffield, Sheffield S3 7HF (UK). E-mail: m.d.ward@sheffield.ac.uk

Abstract

The previously reported complex $[Ru(ttpy)(CN)_3]^-$ [ttpy = 4'(*p*-tolyl)-2,2':6',2"-terpyridine] is conveniently synthesised by reaction of ttpy with $Ru(dmso)_4Cl_2$ to give $[Ru(ttpy)(dmso)Cl_2]$, which reacts in turn with KCN in aqueous ethanol to afford $[Ru(ttpy)(CN)_3]^-$ which was isolated and crystallographically characterised as both its $(PPN)^+$ and K^+ salts. The K^+ salt contains clusters containing three complex anions and three K^+ cations connected by end-on and side-on cyanide ligation to the K^+ ions. The solution speciation behaviour of $[Ru(ttpy)(CN)_3]^-$ was investigated with both Zn^{2+} and K^+ salts in MeCN, a solvent sufficiently non-competitive to allow the added metal cations to associate with the complex anion *via* the externally-directed cyanide lone pairs. UV/Vis spectroscopic titration of $(PPN)[Ru(ttpy)(CN)_3]$ with $Zn(ClO_4)_2$ showed a blue shift of 2900 cm^{-1} in the [1]MLCT absorption manifold due to the 'metallochromism' effect; a series of distinct binding events could be discerned corresponding to formation of 4:1, 1:1 and then 1:3 anion:cation adducts, all with high formation constants, as the titration proceeded. In contrast titration of $(PPN)[Ru(ttpy)(CN)_3]$ with the more weakly Lewis-acidic KPF_6 resulted in a much smaller blue-shift of the [1]MLCT absorptions, and the titration data corresponded to formation of 1:1 and then 2:1 cation:anion adducts with weaker stepwise association constants of the order of 10^4 and then 10^2 M^{-1}. Although association of $[Ru(ttpy)(CN)_3]^-$ resulted in a blue-shift of the [1]MLCT absorptions, the luminescence was steadily quenched, as raising the [3]MLCT level makes radiationless decay *via* a low-lying [3]MC state possible.

1. Introduction

We [1,2] and others [1,3,4] have been investigating the chemistry of luminescent cyanometallates of the $[Ru(bipy)(CN)_4]^{2-}$ type. These are very interesting molecular components to use in supramolecular assemblies for a variety of reasons, including (i) the ability of the externally-directed cyanide groups to form supramolecular assemblies by coordination to other metal cations, or by hydrogen-bonding or halogen-bonding; (ii) the remarkable sensitivity of the spectroscopic and photophysical properties of the metal complex to its environment (solvatochromism and 'metallochromism') which allow applications such as switching and sensing; and (iii) the availability of the CN groups to act as spectroscopic handles in time-resolved IR spectroscopy which allows the excited state dynamic behaviour of complexes containing these fragments to be measured on the picosecond timescale [1].

An obvious extension of this is to investigate related cyanometallates based on different polypyridine ligands, such as $[Ru(tpy)(CN)_3]^-$ which has received considerably less attention than $[Ru(bipy)(CN)_4]^{2-}$. It was first reported in 1996 by Bignozzi, Meyer and co-workers and was prepared by reaction of $[Ru(tpy)Cl_3]$ with excess cyanide, and the solvent dependence of its redox, UV/Vis absorption, and luminescence properties was evaluated [4]. $[Ru(tpy)(CN)_3]^-$ and its simple analogue $[Ru(ttpy)(CN)_3]^-$ [ttpy = 4'-(*p*-tolyl)-2,2':6',2"-terpyridine] were analysed in more detail in 1998 by Scandola and co-workers [5]. In this work it was demonstrated that the photophysical properties of these complexes are superior to those of the $[Ru(tpy)_2]^{2+}$ analogues in some solvents, but that as the energy of the ^{3}MLCT state increased in more hydrogen-bonding solvents, deactivation *via* a close-lying ^{3}MC state became significant, destroying the useful photophysical properties. The effects of different solvents on the electronic properties of $[Ru(tpy)(CN)_3]^-$ have been investigated computationally [6]. Recently Yam and co-workers described how an aza-crown appended derivative of $[Ru(tpy)(CN)_3]^-$ could be used for photometric detection of both cations and amino acids in HPLC separations [7].

In this paper we examine the 'metallochromism' of $[Ru(ttpy)(CN)_3]^-$. On the basis that the photophysical properties of complexes of this nature are strongly dependent on the interaction of the cyanide lone pairs with external electron acceptors such as protons of protic solvents [4], coordination of these cyanides to metal cations should have a comparable or greater effect, as we showed recently with $[Ru(bipy)(CN)_4]^{2-}$ [2f]. Accordingly we describe a new synthetic route to $[Ru(ttpy)(CN)_3]^-$, the crystal structures of two of its salts, and the

results of solution titrations with the metal cations K^+ and Zn^{2+} with analysis of both photophysical properties of the adducts and the solution speciation behaviour.

2. Results and Discussion

2.1 Syntheses and crystal structures

The reported synthesis of $[Ru(ttpy)(CN)_3]^-$, as its potassium and tetrabutylammonium salts, is based on reaction of $[Ru(ttpy)Cl_3]$ with KCN following initial removal of the chloride ions using $AgBF_4$. Following chromatographic purification, $K[Ru(ttpy)(CN)_3]$ was isolated in 32% yield [5]. We have made two modifications to this procedure. Firstly, instead of $[Ru(ttpy)Cl_3]$ as the starting material – which requires the chloride ligands to be removed using either Ag(I) or Tl(I) salts [4,5] – we use the more soluble and labile species $[Ru(ttpy)(dmso)Cl_2]$ [8] which reacts quickly with cyanide in aqueous EtOH to give $[Ru(ttpy)(CN)_3]^-$ as its potassium salt. Secondly, a simplified purification is by cation metathesis, involving precipitation of the anion from aqueous solution with PPN^+Cl^- [PPN^+ is the bis(triphenylphosphine)iminium cation] as reported by Mann and co-workers for preparation of $[PPN]_2[Ru(bipy)(CN)_4]$ [3c]. This affords a precipitate of $(PPN)[Ru(ttpy)(CN)_3]$ that is pure and readily soluble in organic solvents, which is convenient for spectroscopic studies, and avoids the tedious chromatographic purification step.

Crystals of $(PPN)[Ru(ttpy)(CN)_3] \cdot 2CH_2Cl_2$ were grown by slow evaporation of a CH_2Cl_2/hexane solution. The structure is shown in Fig. 1 (see Table 1 for selected bond distances and angles). The complex anion has the expected quasi-octahedral coordination geometry (Fig. 1a), with the major deviation from ideality arising from the limited bite angle of the terpyridyl ligand [the N(1)-Ru(1)-N(3) angle is 157.0°]. As is common with chelating terpyridyl ligands the metal-N bond to the ccentral N atom, Ru(1)–N(2), is shorter than the other two [1.983 Å, compared to 2.070 Å to N(1) and 2.059 Å to N(3)]. The Ru–C distances are all similar and average 2.04 Å. The pendant phenyl ring of the ttpy ligand is near-planar with the coordinated terpyridyl fragment, being twisted by just 8.1° away from the plane of the central pyridyl ring to which it is attached. This facilitates arrangement of the complex anions in a stacked array in which fragments of the ttpy ligands overlap with one another at a distance of *ca.* 3.5 Å, characteristic of aromatic π-stacking (Fig. 1b). In this structure the lone pairs of the cyanide N atoms are not involved in any close contacts with other species, unlike

the case in crystals of $[Ru(bipy)(CN)_4]^{2-}$ which are usually hydrated with numerous CN•••HOH hydrogen-bonding interactions.

Crystals of $K_{0.75}H_{0.25}[Ru(ttpy)(CN)_3]$ were grown by slow evaporation of an aqueous methanol solution of the potassium salt; the structure is shown in Fig. 2 (see Table 1 for selected bond distances and angles). The asymmetric unit contains four crystallographically independent $[Ru(ttpy)(CN)_3]^-$ anions but only three K^+ cations, on the basis of which we assume that the remaining cation is a proton which of course cannot be located but could be associated with a cyanide lone pair or one of the lattice solvent molecules (8 water molecules and 6 MeOH molecules in the asymmetric unit). The quality of the structural determination is limited by the presence of some unresolved disorder which manifests itself in high thermal displacement parameters for the K atoms and some of their coordinated ligands (O and N atoms). Nonetheless it is possible to see reasonably clearly that the crystal structure involves a complex collection of end-on and side-on interactions between cyanide ligands and K^+ cations resulting in formation of cyanide-bridged clusters. We have observed before in related structures how softer metal cations such as K^+ can form side-on interactions with the cyanide ligands of cyanometallate anions, whereas more Lewis-acidic metal cations M', such as lanthanide +3 cations, Li^+ or Ba^{2+}, only form the more usual end-on interactions giving near-linear M–CN–M' bridges [2c, 2f].

Of the four independent Ru(II) complex anions, three [containing Ru(1), Ru(2) and Ru(3)] are associated with the K^+ cations to form discrete K_3Ru_3 clusters (Fig. 2). Of the three Ru(II) units, Ru(3) uses all three of its cyanide ligands to interact with K^+ ions (Fig. 3a) whereas Ru(1) and Ru(2) only use two of their cyanide ligands in this way (Fig. 3b) with the third one [N(4) and N(10), respectively] directed away from the cluster core and involved in non-bonded N•••O contacts shorter than 3Å with lattice water molecules, which indicate the presence of CN•••HOH hydrogen-bonding interactions. The fourth complex anion, containing Ru(4), is not involved in formation of the cluster with K^+ cations but all three cyanide groups are H-bonded to lattice water molecules on the basis of N•••O separations of *ca.* 2.8 Å (Fig. 3c). The coordination geometries around the Ru(II) ions are unremarkable and similar to one another.

2.2 Solution spectroscopic properties: metallochromism in UV/Vis and luminescence spectra, and speciation with other metal cations

The solvatochromism of $[Ru(tpy)(CN)_3]^-$ and $[Ru(ttpy)(CN)_3]^-$ have been investigated in detail previously [4,5]. The complexes show very similar UV/Vis spectroscopic behaviour,

with a manifold of closely-spaced [1]MLCT absorptions peaking in the 500 – 600 nm region in non hydrogen-bonding solvents, which blue shift in protic solvents up to a limit of 427 nm in water. This is similar in principle to the solvatochromic behaviour of $[Ru(bipy)(CN)_4]^{2-}$ [4] but the solvatochromic shift in the tpy-based complexes is smaller because of the presence of only three cyanide groups rather than four.

We were interested to examine the 'metallochromism' of $[Ru(ttpy)(CN)_3]^-$, *i.e.* the extent to which the electronic spectral properties can be altered in the presence of metal cations which interact with the cyanide lone pairs in a relatively non-competitive solvent (*i.e.* one that does not prevent the Ru–CN•••M^{n+} by coordinating strongly to the metal ion, or hydrogen bonding to the cyanides, or both). With $[Ru(bipy)(CN)_4]^{2-}$ in MeCN we found that Lewis-acidic metal cations from groups 1 and 2, as well as Zn^{2+}, interacted with the cyanide lone pairs to give very substantial increases in the energy of [1]MLCT absorption and [3]MLCT emission spectra [2f]. For example the lowest energy [1]MLCT absorption of $(PPN)_2[Ru(^tBu_2bipy)(CN)_4]$ shifted from 529 nm in MeCN to 370 nm in the presence of excess $Zn(BF_4)_2$ (a blue shift of *ca.* 8000 cm^{-1}); at the same time the [3]MLCT emission shifted from *ca.* 800 nm (very weak, $\tau \approx 12$ ns) up to 537 nm, a blue shift of 6000 cm^{-1}, with a concomitant dramatic increase in intensity and lifetime (730 ns). Similar results were obtained with other simple metal salts, with the magnitude of the effect generally depending on the Lewis-acidity of the metal cation concerned [2f].

Accordingly we performed a spectroscopic titration whereby portions of $Zn(ClO_4)_2$ from a standard solution were added to a solution of $(PPN)[Ru(ttpy)(CN)_3]$ in MeCN (*ca.* 5 x 10^{-5} M) and the effect on UV/Vis absorption, and visible luminescence, measured. The resulting changes in UV/Vis absorption are shown in Figure 4 and reveal some interesting solution speciation behaviour. In neat MeCN the main [1]MLCT absorption maximum of $(PPN)[Ru(ttpy)(CN)_3]$ is at 500 nm, with a low-energy shoulder at *ca.* 540 nm. As portions of $Zn(ClO_4)_2$ are added the [1]MLCT absorption maximum blue-shifts, as expected, with the Zn(II) ions coordinated to cyanide groups acting as electron-withdrawing groups and therefore giving the same spectroscopic response as a protic solvent containing δ+ H atoms. At the end of the titration, after addition of > 6 equivalents of $Zn(ClO_4)_2$, the [1]MLCT maximum was blue-shifted to 433 nm, a blue-shift of *ca.* 2900 cm^{-1}. In addition, there are pronounced increases in absorbance in the UV region in the regions around 330 nm and 300 nm, and a decrease in absorbance for the closely-spaced series of peaks between 250 and 300 nm.

The changes in the electronic spectra as $Zn(ClO_4)_2$ is added are not smooth however but show several different domains from which we can extract interesting information about speciation in solution. Changes in absorbance as a function of added $Zn(ClO_4)_2$, at selected wavelengths where the absorbance changes are large, are shown in Fig. 5. At the early stages of the titration there are substantial changes in absorbance – increases at 420 and 300nm, and a decrease at 284 nm – which are linear with amount of added $Zn(ClO_4)_2$ until about 0.25 equivalents has been added, at which point there is a sudden gradient change. The implication of this is that a 4:1 $[Ru(ttpy)(CN)_3]^-:Zn^{2+}$ adduct forms at the strong binding limit, *i.e.* with individual stepwise 1:1 binding constants that are high compared to the reciprocal of the concentration ($\gg 2 \times 10^4$ M^{-1}). Given that stepwise binding constants for a range of metal cations to $[Ru(^tBu_2bipy)(CN)_4]^{2-}$ in MeCN were in the range $10^4 - 10^6$ M^{-1} this is reasonable. The 4:1 cation:anion ratio suggests that a tetrahedral Zn(II) complex forms with four bulky cyanoruthenate anions coordinated to each Zn(II) ion *via* linear Ru–CN–Zn bridges. The calculated 4:1 $[Ru(ttpy)(CN)_3]^-:Zn^{2+}$ binding constant used in the fit shown in Fig. 5 is 10^{26} M^{-4} (*i.e.* averaging greater than 10^6 M^{-1} for each individual binding event); we emphasise that this is an order of magnitude estimate at best.

As the titration proceeds past this point there is a clear discontinuity in the absorbance *vs.* $[Zn^{2+}]$ curves with the gradient diminishing but the curves staying approximately linear until the ratio reaches 1:1. This second domain therefore corresponds to rearrangement of the 4:1 $[Ru(ttpy)(CN)_3]^-:Zn(II)$ adduct – formed when there is a deficiency of Zn^{2+} ions – to a 1:1 adduct $\{Zn[Ru(ttpy)(CN)_3]\}^+$ in which, presumably, those coordination sites around the Zn^{2+} ion that are not occupied by cyanide ligands are occupied by MeCN solvent molecules, water molecules [since the $Zn(ClO_4)_2$ is hydrated] and/or perchlorate anions. The calculated best fit (as used in Figure 5) for this 1:1 binding constant is $\approx 10^9$ M^{-1} (again, an order-of-magnitude estimate). As the titration proceeds further and $Zn(ClO_4)_2$ is present in a larger excess there is an additional gradient change at an anion:cation ratio of 1:3, which presumably corresponds to a situation in which all three externally-directed cyanide ligands interact with a different Zn(II) ion ($K \approx 10^{21}$ M^{-3}). The approximate linearity of the absorbance *vs.* $[Zn^{2+}]$ plot in all three domains, *viz.* formation of the 4:1, 1:1 and then 1:3 anion:cation adducts, means that all individual binding constants are in the strong binding limit with respect to the concentration used. After formation of the 1:3 adduct there is an additional discontinuity in the data (Fig. 5) corresponding to formation of a final species in which there are >3 Zn(II) ions around each $[Ru(ttpy)(CN)_3]^-$ anion but the stoichiometry of this cannot be determined. Fits of the absorbance data at three different wavelengths to this set of equilibria, assuming high binding

constants with respect to the concentration used, are quite convincing and are shown in Fig. 5. It might be expected that binding several Zn(II) ions around a single $[Ru(ttpy)(CN)_3]^-$ centre would result in rapidly decreasing stepwise association constants for electrostatic reasons, but if the Zn(II) ions retain their perchlorate anions as ligands and bind as ion-pairs then the buildup of positive charge will be prevented [2f].

An identical experiment using $Ba(ClO_4)_2$ gave similar results although the changes in gradient at the 4:1, 1:1 and 1:3 stoichiometry points were not so clear; possibly the weaker Lewis acidity of Ba(II) compared to Zn(II) means that the binding is no longer completely at the strong limit.

We then performed a similar experiment using KPF_6 as the source of the metal cation to bind to the cyanide groups to see how a more weakly Lewis acidic metal cation would affect the behaviour of the $[Ru(ttpy)(CN)_3]^-$ group. Again, at the start of the titration we observed the main [1]MLCT absorption of $[Ru(ttpy)(CN)_3]^-$ in MeCN at 500 nm with a shoulder at about 540 nm. As portions of KPF_6 were added we again observed a blue shift of these transition but the shift was both lower in magnitude [indicative of a weaker electron withdrawing effect of K^+ ions compared to Zn(II) ions] and slower to develop (indicative of weaker cation / anion binding). At the end of the titration the [1]MLCT maximum had blue-shifted by just 3 nm to 497 nm with a slight decrease in intensity (Fig. 6). The main changes in the absorption spectrum are an increase in absorbance between 400 and 450 nm, a similar increase in absorbance at around 350 nm, and a decrease in absorbance in the UV region between 250 nm and 300 nm, all in agreement with what was observed during the titration with $Zn(ClO_4)_2$. A plot of absorbance change as a function of added KPF_6 shows quite simple behaviour however, in contrast to what was observed with $Zn(ClO_4)_2$, with clear evidence for two binding processes with the first being much stronger than the second. Taking the change in absorbance at the wavelength where the change is greatest, *viz* at 280 nm, the titration curve can be fitted to a 1:2 anion:K^+ isotherm with stepwise microscopic binding constants of *ca.* 10^4 M^{-1} and 10^3 M^{-1} (Fig. 7). As these values are correlated with each other significant changes in one can be compensated by changes in the other to give a comparably good fit to the observed data, so these are order of magnitude estimates only. The general pattern is clear: a 1:1 $[Ru(ttpy)(CN)_3]^-$/K^+ adduct forms in MeCN with a high binding constant of the order of 10^4 M^{-1}, and subsequent binding of a second equivalent of K^+ has an association constant about one orders of magnitude less. Thus, both the extent of association and the degree of perturbation of the electronic spectrum that occurs on binding are less with K^+ than with Zn^{2+}, in agreement with their relative Lewis acidity.

The effect of association of $[Ru(ttpy)(CN)_3]^-$ complex anions with Zn^{2+} or K^+ cations in MeCN on the luminescence behaviour of the chromophore was disappointing however. The weak emission band at *ca.* 700 nm simply reduced in intensity as the titrations proceeded until by the end of the titration it had disappeared. Although a blue-shift in the emission maximum is expected, in agreement with the blue shifts in the ^{1}MLCT absorption maxima, it was shown by Scandola and co-workers that, as the emission maximum moves to higher energy, it substantially reduces in intensity and lifetime due to thermal equilibration with the higher-lying ^{3}MC (d-d) excited state whose decay is fast and radiationless [5]. Therefore the change in luminescence as the ^{3}MLCT energy varies is exactly the inverse of what is normally expected on the basis of the 'energy-gap law'. All we see in the luminescence spectra during the titration is the diminishing amount of luminescence from the free, uncomplexed $[Ru(ttpy)(CN)_3]^-$ anion in MeCN; this residual and (relatively) intense luminescence obscures any evidence for the very much weaker high-energy emission component that might be expected.

3. Conclusions

We have described a simple new synthesis of the complex anion $[Ru(ttpy)(CN)_3]^-$ which is potentially extendable to any substituted terpyridyl-type ligand, and reported the first crystal structures of this chromophore. In a non-competitive solvent (MeCN) $[Ru(ttpy)(CN)_3]^-$ aggregates with added Zn^{2+} ions in a series of well-defined steps, all with high association constants, to give 4:1, 1:1 and then 1:3 anion:cation adducts. The more weakly Lewis-acidic metal cation K^+ also interacted with $[Ru(ttpy)(CN)_3]^-$ in MeCN but more weakly for simple electrostatic reasons, showing formation of 1:1 and then 1:2 anion:cation adducts with association constants for the two steps of the order of 10^4 and then 10^3 M^{-1}. Interaction of the cyanide lone pairs with the external metal cations results in modest blue-shifts of the ^{1}MLCT absorption maximum in the UV/Vis spectrum, with Zn^{2+} inducing a much larger metallochromic shift than K^+. However the associated increase in the ^{3}MLCT energy resulted in quenching of the luminescence due to thermal equilibration with a non-emissive ^{3}MC state.

4. Experimental

4.1 Materials and instrumentation

The ligand ttpy [9] and the metal complex $Ru(dmso)_4Cl_2$ [10] were prepared according to published procedures. The following instruments were used for spectroscopic characterisation and analysis: UV/Vis spectra, a Cary-50 spectrophotometer; luminescence spectra, a Jobin-Yvon Fluoromax 4 fluorimeter; Electrospray mass spectra, a Micromass LCT instrument; NMR spectra, a Bruker Avance-III 400 instrument. Association constants from the UV/Vis titrations were calculated using procedures and home-written software that has been described previously [11].

4.2 Preparation of K[Ru(ttpy)(CN)₃] and (PPN)[Ru(ttpy)(CN)₃]

Part I: Synthesis of [Ru(ttpy)(dmso)Cl₂] **A**. A mixture of $Ru(dmso)_4Cl_2$ (306 mg, 0.632 mmol) and ttpy (204 mg, 0.632 mmol) ligand in ethanol (50 cm³) was heated to reflux overnight with stirring. The mixture was cooled to room temperature and the solvent removed by evaporation to give a purple residue of crude $[Ru(ttpy)(dmso)Cl_2]$ which was used directly in the next step. ^{1}H NMR (CDCl₃): δ 8.73 (s, 2H; ttpy) 8.70 (d, 2H; ttpy), 8.65 (d, 2H; ttpy), 7.82 (ddd, 2H; ttpy), 7.75 (d, 2H; ttpy), 7.30 (ddd, 2H; ttpy), 7.25 (d, 2H; ttpy), 2.85 (s, 3H; dmso) 1.58 (s, 3H; Me on ttpy). ESMS: *m/z* 453 $[M - dmso]^+$.

Part II: Synthesis of K[Ru(ttpy)(CN)₃] **B**. A mixture of complex **A** (250 mg, 0.436 mmol) and potassium cyanide (170 mg, 2.61 mmol, six equivalents) in aqueous ethanol (50 cm³, 1:1 v/v) was heated to reflux overnight with stirring. The mixture was then cooled to room temperature and evaporated to dryness. This crude product (contain excess KCN) was used directly in the next step; X-ray quality crystals were grown by slow evaporation of a solution in aqueous methanol. ^{1}H NMR (D₂O): δ 8.70 (s, 2H) 8.53 (d, 2H) 8.33 (d, 2H) 7.42 (ddd, 2H) 7.15 (d, 2H) 7.05 (ddd, 2H) 6.32 (d, 2H), 1.70 (s, 3H). ESMS: *m/z* 503 $[M - K^+]^-$.

Part III: Synthesis of PPN[Ru(ttpy)(CN)₃] **C**. The complete yield of **B** from the above reaction was dissolved in the minimum amount of hot water. Bis(triphenylphosphine)iminium chloride (0.303 g, 0.528 mmol, 1.2 equivalents assuming 100% yield in the above reaction) was dissolved in water (50 cm³) at 80˚C. The warm aqueous solution containing complex **B** was added drop wise to the warm solution of PPNCl resulting in immediate precipitation of

complex **C**. The hot suspension was filtered over celite, washed with hot water and dried. The precipitate was then collected by washing the celite with dichloromethane and acetonitrile and the resulting purple solution was evaporated to dryness. Overall yield of **C**: 63%. ^{1}H NMR (CDCl$_3$): δ 8.78 (s ,2H), 8.72 (d, 2H; ttpy), 8.15 (d, 2H; ttpy) 7.90 (ddd, 2H; ttpy) 7.85 (d, 2H; ttpy) 7.70 (m, 36H; phenyl rings of PPN$^+$), 7.41 (ddd, 2H; ttpy) 7.32 (d, 2H; ttpy) 1.93 (s 3H Me on ttpy). ESMS: *m/z* 503 [*M* – PPN$^+$]$^-$. Anal. Found: C, 58.8; H, 4.3; N, 7.6%. C$_{61}$H$_{47}$N$_7$RuP$_2$•3CH$_2$Cl$_2$ requires: C, 59.3; H, 4.1; N, 7.6%.

4.3 X-ray crystallography

X-ray crystallographic data are summarised in Table 2. In each case a suitable crystal was coated with hydrocarbon oil and attached to the tip of a glass fibre and transferred to a Bruker APEX-2 CCD diffractometer (graphite monochromated Mo-Kα radiation, λ = 0.71073 Å) under a stream of cold N$_2$. After collection and integration the data were corrected for Lorentz and polarisation effects and for absorption by semi-empirical methods (SADABS) [12] based on symmetry-equivalent and repeated reflections. The structures were solved by direct methods or heavy atom Patterson methods and refined by full matrix least squares methods on F^2. Hydrogen atoms were placed geometrically and refined with a riding model and with U_{iso} constrained to be 1.2 (1.5 for methyl groups) times U_{eq} of the carrier atom. Structures were solved and refined using the SHELX suite of programs [13]. Significant bond distances and angles for the structures of the metal complexes are in Table 1.

Supplementary data

CCDC 760845 and 760846 contain the supplementary crystallographic data for this paper. These data can be obtained free of charge from http://www.ccdc.cam.ac.uk/conts/retrieving.html, or from the Cambridge Crystallographic Data Centre, 12 Union Road, Cambridge CB2 1EZ, UK; fax: (+44) 1223 336033; or email: deposit@ccdc.cam.ac.uk.

References

[1]   M. D. Ward, Coord. Chem. Rev. 250 (2006) 3128.

[2]   (a) G. M. Davies, S. J. A. Pope, H. Adams, S. Faulkner, M. D. Ward, Inorg. Chem. 44 (2005) 4656,

(b) H. Adams, W. Z. Alsindi, G. M. Davies, M. B. Duriska, T. L. Easun, H. E. Fenton, J.-M. Herrera, M. W. George, K. L. Ronayne, X.-Z. Sun, M. Towrie, M. D. Ward, Dalton Trans. (2006) 39.

(c) J.-M. Herrera, S. J. A. Pope, H. Adams, S. Faulkner, M. D. Ward, Inorg. Chem. 45 (2006) 3895.

(d) S. G. Baca, H. Adams, D. Sykes, S. Faulkner, M. D. Ward, Dalton Trans. (2007) 2419.

(e) J.-M. Herrera, S. J. A. Pope, A. J. H. M. Meijer, T. L. Easun, H. Adams, W. Z. Alsindi, X.-Z. Sun, M. W. George, S. Faulkner, M. D. Ward, J. Am. Chem. Soc. 129 (2007) 11491.

(f) T. Lazarides, T. L. Easun, C. Veyne-Marti, W. Z. Alsindi, M. W. George, N. Deppermann, C. A. Hunter, H. Adams, M. D. Ward, J. Am. Chem. Soc. 129 (2007) 4014.

(g) S. G. Baca, H. Adams, C. S. Grange, A. P. Smith, I. Sazanovich, M. D. Ward, Inorg. Chem. 46 (2007) 9779.

(h) S. Derossi, H. Adams, M. D. Ward, Dalton Trans. (2007) 33.

(i) S. G. Baca, S. J. A. Pope, H. Adams, M. D. Ward, Inorg. Chem. 47 (2008) 3736.

(j) S. Derossi, L. Brammer, C. A. Hunter, M. D. Ward, Inorg. Chem. 48 (2009) 1666.

(k) S. Derossi, S. G. Baca, T. A. Miller, H. Adams, J. C. Jeffery, M. D. Ward, Inorg. Chim. Acta 362 (2009) 1282.

[3]   (a) J. L. Habib Jiwan, B. Wegewijs, M. T. Indelli, F. Scandola, S. E. Braslavsky, Recl. Trav. Chim. Pays-Bas 114 (1995) 542.

(b) M. Kovács, A. Horvath, Inorg. Chim. Acta 335 (2002) 69.

(c) J. K. Evju, K. R. Mann, Chem. Mater. 11 (1999) 1425.

(d) S. L. Howell, K. C. Gordon, J. J. McGarvey, J. Phys. Chem. A, 109 (2005) 2948.

(e) R. Argazzi, C. A. Bignozzi, M. Yang, G. M. Hasselmann, G. J. Meyer, Nano Lett. 2 (2002) 625.

(f) T. Megyes, G. Schubert, M. Kovács, T. Radnai, T. Grósz, I. Bakó, I. Pápai, A. Horváth, J. Phys. Chem. A 107 (2003) 9903.

(g) G. Bergamini, C. Saudan, P. Ceroni, M. Maestri, V. Balzani, M. Gorka, S.-K. Lee, J. van Heyst, F. Vögtle, J. Am. Chem. Soc. 126 (2004) 16466.

(h) F. Pina, A. J. Parola, Coord. Chem. Rev. 185-186 (1999) 149.

[4]   C. J. Timpson, C. A. Bignozzi, B. P. Sullivan, E. M. Kober, T. J. Meyer, J. Phys. Chem. 100 (1996) 2915.

[5]   M. T. Indelli, C. A. Bignozzi, F. Scandola, J.-P. Collin, Inorg. Chem. 37 (1998) 6084.

[6]   M. Franco, K. Araki, R. C. Rocha, H. E. Toma, J. Solution Chem. 29 (2000) 667.

[7]   M.-J. Li, B. W.-K. Chu, V. W.-W. Yam, Chem. Eur. J. 12 (2006) 3528.

[8]   (a) R. Ziessel, V. Grosshenny, M. Hissler, C. Stroh, Inorg. Chem. 43 (2004) 4262.

(b) T. Norrby, A. Börje, B. Åkermark, L. Hammarström, J. Alsins, K. Lashgari, R. Norrestam, J. Mårtensson, G. Stenhagen, Inorg. Chem. 36 (1997) 5850.

[9]   F. Tessore, D. Roberto, R. Ugo, M. Pizzotti, Inorg. Chem. 44 (2005) 8971.

[10]   G. Canard, C. Piguet, Inorg. Chem. 46 (2007) 3511.

[11]   T. Lazarides, T. L. Easun, C. Veyne-Marti, W. Z. Alsindi, M. W. George, N. Deppermann, C. A. Hunter, H. Adams, M. D. Ward, J. Am. Chem. Soc. 129 (2007) 4014.

[12]   G. M. Sheldrick: SADABS, A program for absorption correction with the Siemens SMART area-detector system; University of Göttingen (1996).

[13]   G. M. Sheldrick: SHELXS-97 and SHELXL-97, programs for crystal structure solution and refinement; University of Göttingen (1997).

Table 1. Selected bond distances (Å) for the two crystal structures.

K₃H[Ru(ttpy)(CN)₃]₄•6MeOH•8H₂O

Ru(1)-N(2)	1.992(10)	K(1)-N(11)	2.744(10)
Ru(1)-C(24)	2.009(14)	K(1)-O(3S)	2.758(11)
Ru(1)-C(25)	2.030(14)	K(1)-O(1W)	2.87(2)
Ru(1)-C(23)	2.049(14)	K(1)-O(2W)	2.903(18)
Ru(1)-N(3)	2.072(11)	K(1)-O(2W')	2.904(18)
Ru(1)-N(1)	2.079(12)	K(1)-N(16)	2.948(14)
Ru(2)-N(8)	1.997(11)	K(1)-O(3W)	2.966(19)
Ru(2)-C(48)	2.040(16)	K(1)-N(17)	2.97(3)
Ru(2)-C(50)	2.040(16)	K(1)-C(73)	3.313(15)
Ru(2)-N(9)	2.068(10)	K(2)-N(17)	2.578(15)
Ru(2)-C(49)	2.085(17)	K(2)-N(12)	2.834(13)
Ru(2)-N(7)	2.117(10)	K(2)-N(11)	2.85(2)
Ru(3)-N(14)	1.968(12)	K(2)-N(6)	2.902(11)
Ru(3)-C(75)	2.050(17)	K(2)-N(5)	2.94(3)
Ru(3)-C(74)	2.056(18)	K(2)-C(23)	3.150(13)
Ru(3)-N(13)	2.068(11)	K(2)-C(50)	3.214(15)
Ru(3)-C(73)	2.073(17)	K(2)-O(8W')	3.25(3)
Ru(3)-N(15)	2.097(11)	K(2)-O(8W)	3.25(3)
Ru(4)-N(20)	1.976(10)	K(2)-C(24)	3.320(15)
Ru(4)-C(99)	1.992(12)	K(2)-C(49)	3.391(18)
Ru(4)-C(100)	2.008(17)	K(3)-O(6W)	2.807(17)
Ru(4)-C(98)	2.015(17)	K(3)-O(7W')	2.938(19)
Ru(4)-N(21)	2.077(12)	K(3)-O(7W)	2.941(19)
Ru(4)-N(19)	2.087(12)	K(3)-N(5)	2.95(2)
		K(3)-O(7S)	3.06(8)
		K(3)-N(18)	3.176(16)
		K(3)-O(6S)	3.20(4)
		K(3)-C(74)	3.283(16)
		K(3)-C(75)	3.388(17)

(PPN)[Ru(ttpy)(CN)₃]•2CH₂Cl₂

Ru(1)-N(2)	1.983(4)
Ru(1)-C(24)	2.025(5)
Ru(1)-C(23)	2.048(5)
Ru(1)-C(25)	2.056(5)
Ru(1)-N(3)	2.059(4)
Ru(1)-N(1)	2.070(4)

Table 2. Crystal, data collection and refinement data for the two crystal structures.

Complex	(PPN)[Ru(ttpy)(CN)$_3$] •2CH$_2$Cl$_2$	K$_3$H[Ru(ttpy)(CN)$_3$]$_4$ •6MeOH•8H$_2$O
Formula	C$_{63}$H$_{51}$Cl$_4$N$_7$P$_2$Ru	C$_{106}$H$_{109}$K$_3$N$_{24}$O$_{14}$Ru$_4$
Molecular weight	1210.92	2464.75
Crystal system	Triclinic	Triclinic
Space group	$P–1$	$P–1$
T, K	150(2)	150(2)
a, Å	11.1031(3)	13.4835(10)
b, Å	16.9830(5)	13.6033(8)
c, Å	17.8345(5)	29.9723(19)
α,°	103.166(2)	91.953(4)
β,°	101.555(2)	94.913(5)
γ,°	106.501(2)	94.231(5)
V, Å^3	3010.54(15)	5457.9(6)
Z	2	2
ρ, g cm^{-3}	1.336	1.500
Crystal size, mm^3	0.47 x 0.22 x 0.04	0.14 x 0.03 x 0.03
μ, mm^{-1}	0.536	0.730
Unique data, restraints, parameters	17696, 3, 721	16403, 32, 1317
Final R1, $wR2^a$	0.081, 0.266	0.093, 0.277

a The value of R1 is based on selected data with $I > 2s(I)$; the value of wR2 is based on all data.

Captions for Figures

Fig. 1   Molecular structure of (PPN)[Ru(ttpy)(CN)$_3$]•2CH$_2$Cl$_2$. Top: an ORTEP view (thermal ellipsoids at 40% probability level) showing the atomic labelling scheme; bottom, a view showing the aromatic stacking between adjacent complex anions.

Fig. 2   The cation / anion cluster in the crystal structure of K$_3$H[Ru(ttpy)(CN)$_3$]$_4$ •6MeOH•8H$_2$O, involving three [Ru(ttpy)(CN)$_3$]$^-$ anions and three K$^+$ cations. Coordinated solvent molecules (water and methanol) on the K$^+$ ions are omitted for clarity.

Fig. 3   Details of the crystal structure of K$_3$H[Ru(ttpy)(CN)$_3$]$_4$•6MeOH•8H$_2$O. (a): The coordination environment around the cyanide ligands attached to Ru(3). (b): The coordination environment around the cyanide ligands attached to Ru(1). (c): The coordination environment around the cyanide ligands attached to Ru(4). In (b) and (c) the dotted lines denoting OH•••N hydrogen bonding interactions between cyanide ligands and lattice water molecules.

Fig. 4   Changes in the UV/Vis absorption spectrum of (PPN)[Ru(ttpy)(CN)$_3$] in MeCN (10^{-5} M) during titration with Zn(ClO$_4$)$_2$. The limiting (first and last) spectra are shown in bold and the directions of the most obvious changes are shown with arrows. The inset is an expansion of the MLCT absorption region.

Fig. 5   Plots of changes in absorbance as a function of added Zn^{2+} during the titration depicted in Fig. 4, taken at (i) 330 nm, (ii) 420 nm, and (iii) 284 nm. The solid line is the best fit based on the calcuated values for the formation constants given in the main text.

Fig. 6   Changes in the UV/Vis absorption spectrum of (PPN)[Ru(ttpy)(CN)$_3$] in MeCN (10^{-5} M) during titration with KPF$_6$. The limiting (first and last) spectra are shown in bold and the directions of the most obvious changes are shown with arrows. The inset is an expansion of the MLCT absorption region.

Fig. 7   Plot of changes in absorbance at 280 nm as a function of added KPF_6 during the titration depicted in Fig. 6.

Scheme 1   Sketches of the possible structures of the 4:1, 1:1 and 1:3 $[Ru(ttpy)(CN)_3]^-$:Zn^{2+} adducts formed during titration of (PPN) $[Ru(ttpy)(CN)_3]$ with $Zn(ClO_4)_2$ in MeCN.
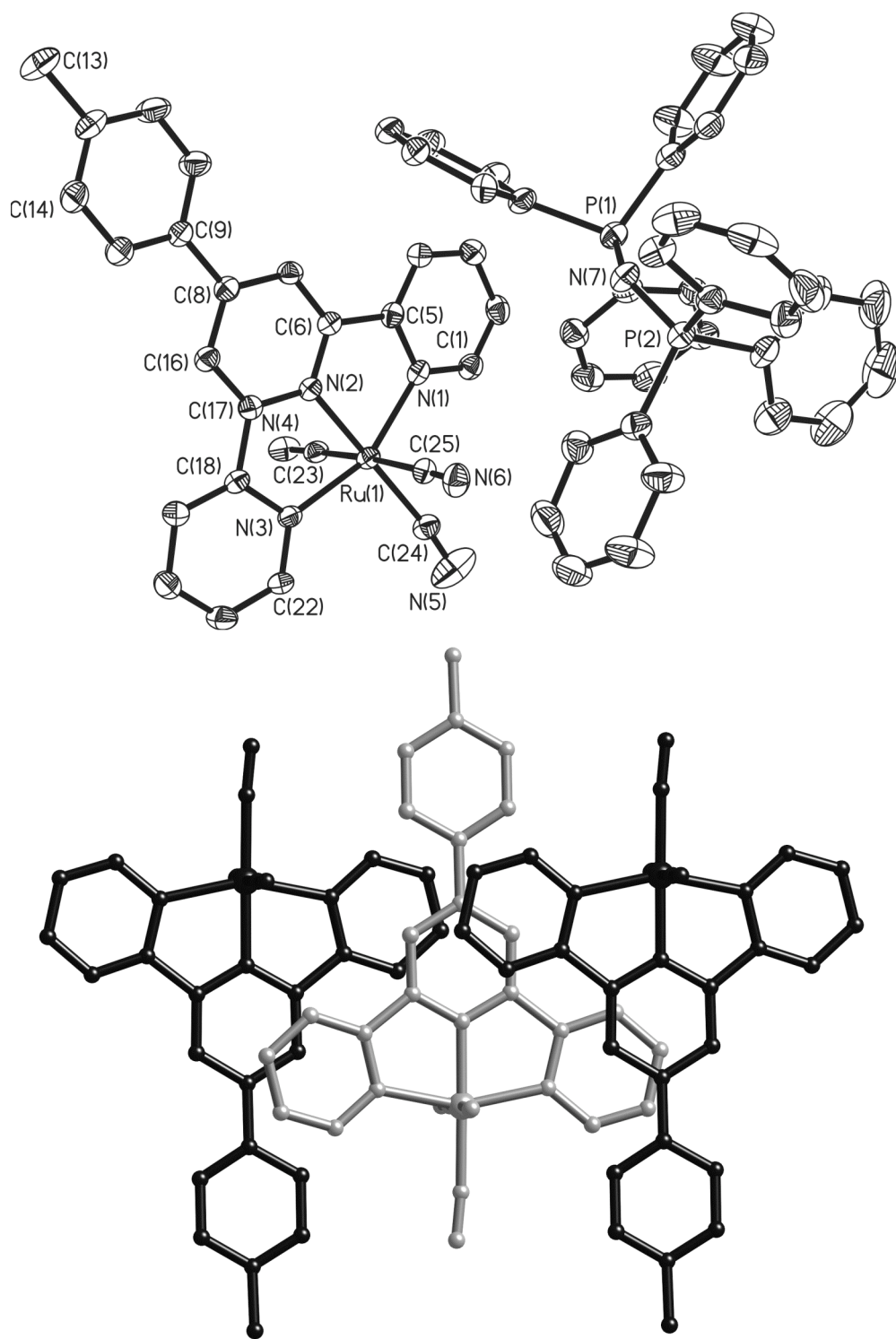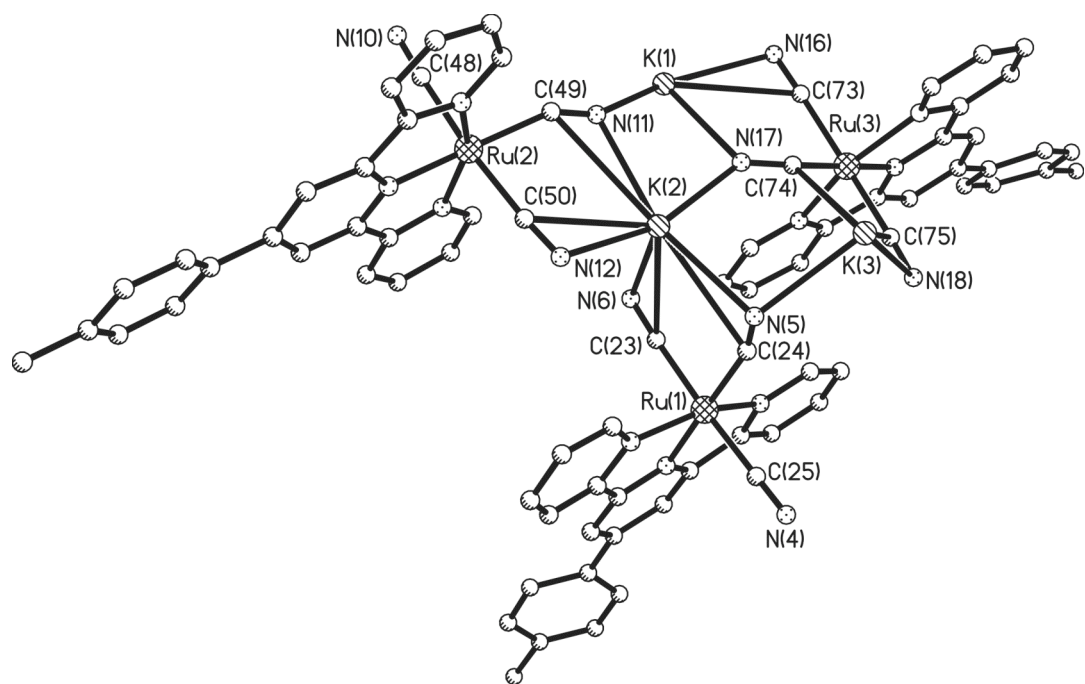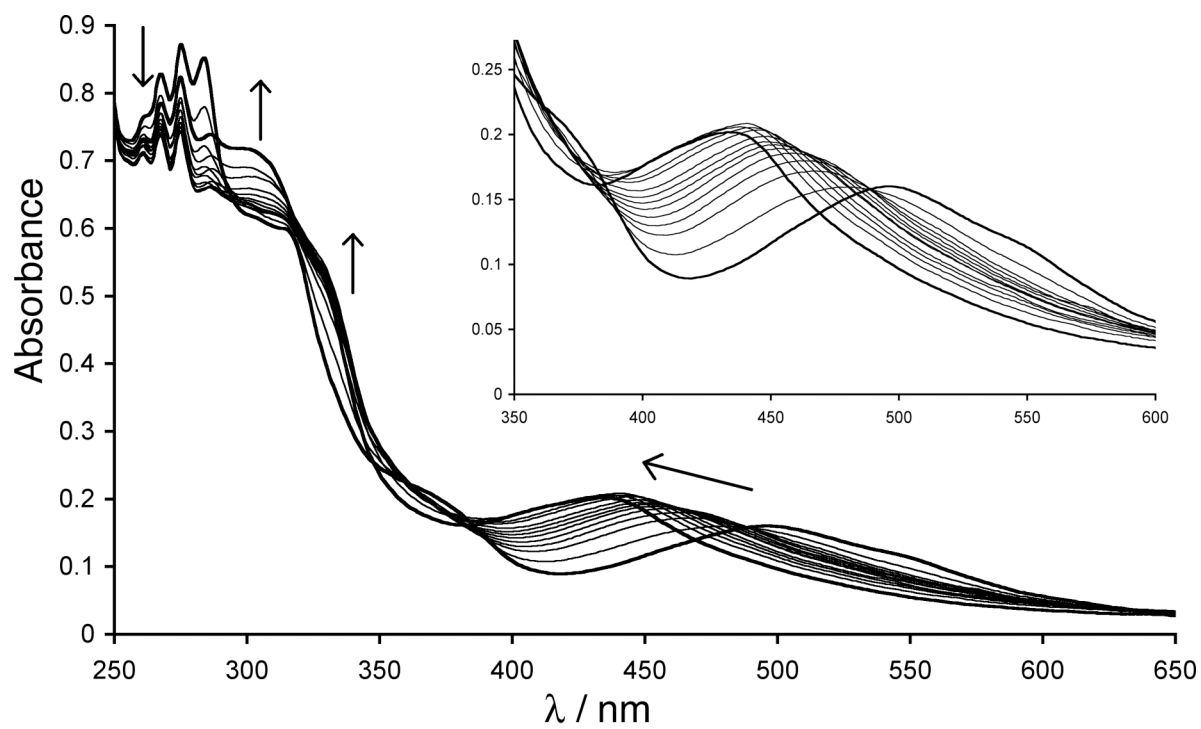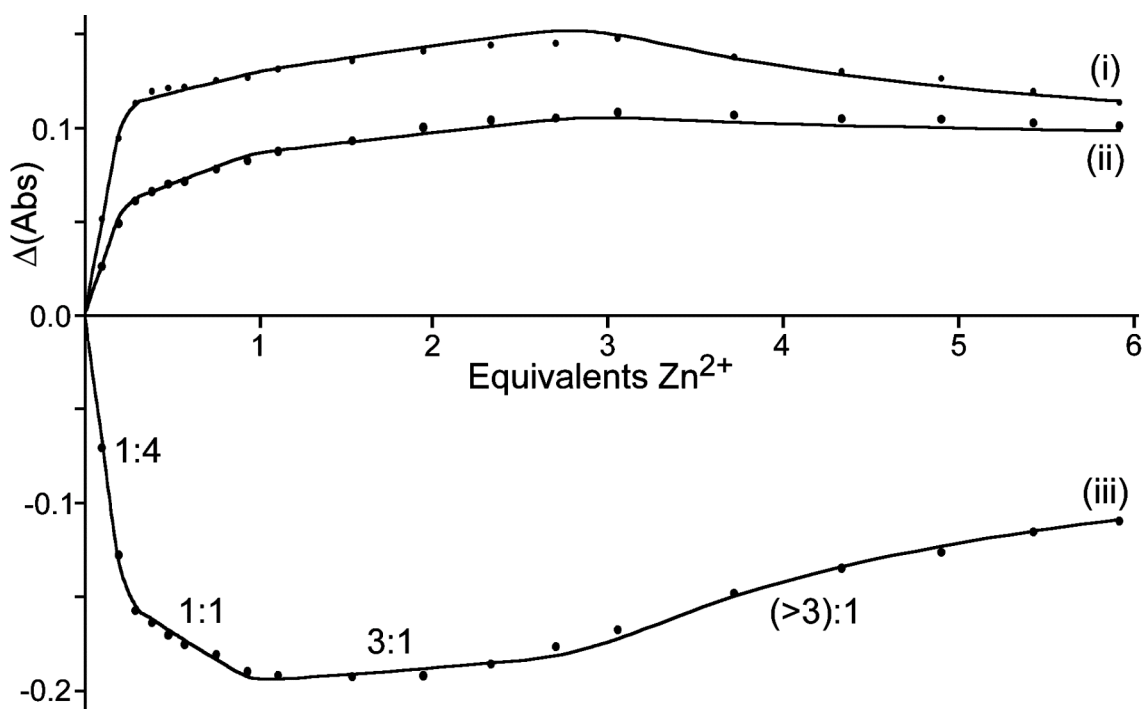
Figure 1

Figure 2

Figure 3

Figure 4

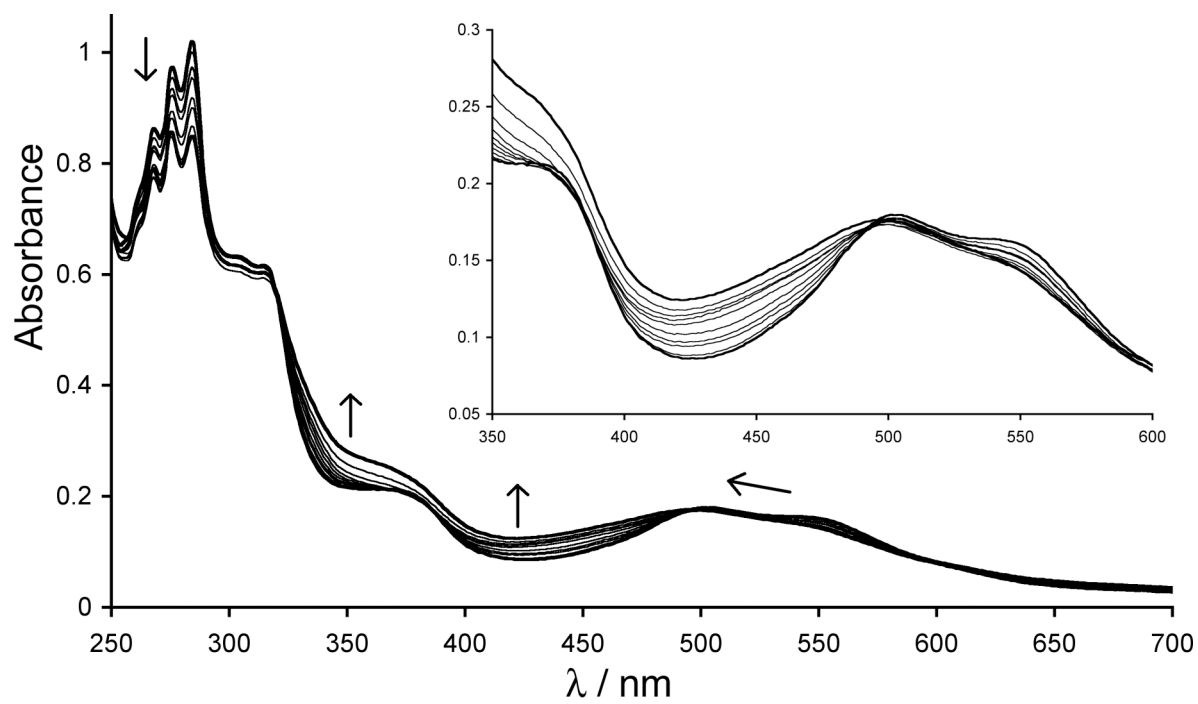Figure 5

Figure 6

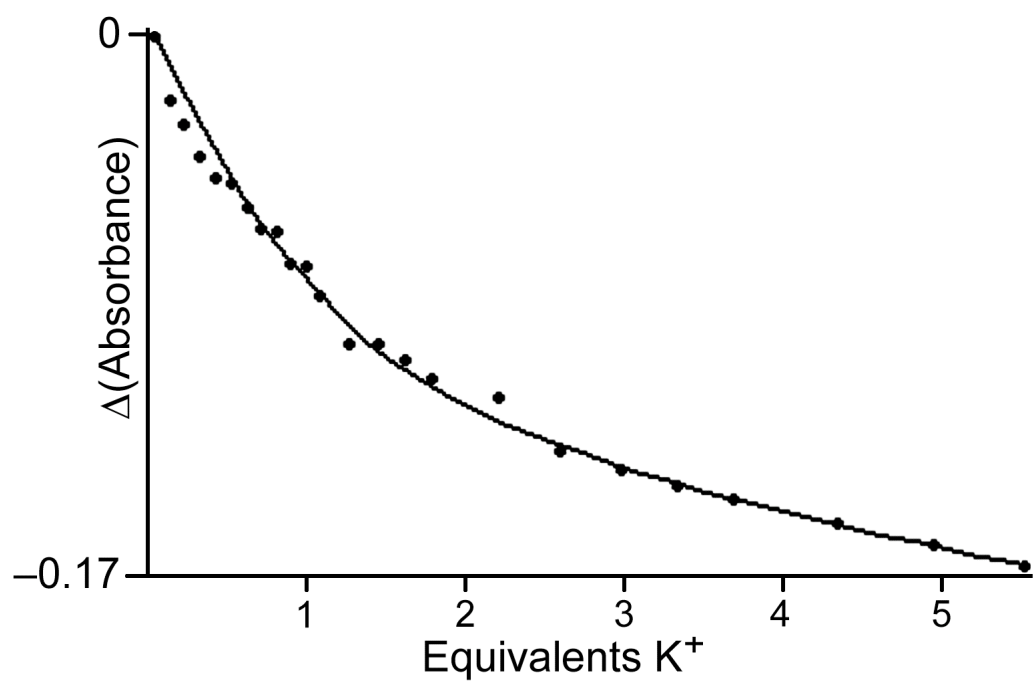

Figure 7

Scheme 1